Proxy stripping: a performance-enhancing technique for optical metropolitan area ring networks

Martin Herzog

Telecommunication Networks Group, Technical University Berlin, 10587 Berlin, Germany

herzog@tkn.tu-berlin.de

http://www.tkn.tu-berlin.de/~herzog/

Stefan Adams

Max Planck Institute for Mathematics in the Sciences, 04103 Leipzig, Germany

adams@mis.mpg.de

Martin Maier

Institut National de la Recherche Scientifique (INRS), Montréal, Québec H5A 1K6, Canada

maier@ieee.org

Metropolitan area ring networks can be categorized into metro edge and metro core rings. The traffic characteristics of metro edge and metro core rings are quite different. While metro edge rings exhibit a strongly hubbed traffic pattern (hot spots), traffic demands in metro core rings are much more uniform. We examine the throughput-delay performance of a buffer insertion ring with destination stripping and shortest path routing, which is the favored network type in the new high-performance standard for metropolitan area ring networks, IEEE 802.17 Resilient Packet Ring (RPR), and we investigate the ring's performance limitations under different traffic characteristics by means of analysis and simulation. Our probabilistic analysis considers arbitrary propagation delays, packet length distributions, and traffic matrices. In our numerical investigations we consider uniform, hot-spot, symmetric, and asymmetric traffic demands. Our findings show that the throughput-delay performance of buffer insertion rings deteriorates significantly under hot-spot traffic compared with uniform traffic. To mitigate this drawback, we propose and investigate the novel performance-enhancing proxy-stripping technique. Proxy stripping is used by a subset of ring nodes to send traffic across shortcuts of a dark-fiber star subnetwork. Our results show that proxy stripping dramatically improves the throughput-delay performance of buffer insertion rings not only under uniform traffic but also, in particular, under hot-spot traffic. Finally, we address the trade-offs of the proxy-stripping technique. © 2005 Optical Society of America

OCIS codes: 060.4250, 060.4510.

1. Introduction

A plethora of next-generation metropolitan area networks with various topologies, access protocols, and fairness protocols have been proposed and investigated to date [1]. In this paper we focus on metro networks with a ring topology, since rings are typically found at the metro level of today's networks [2]. Metro rings can be either asynchronous (e.g., token ring) or synchronous (e.g., empty slot) networks. In this paper we focus on asynchronous buffer insertion rings but note that our results can be extended to any type of metro ring network in a straightforward fashion. The buffer insertion ring is the favored network type in the new high-performance standard for metropolitan area ring networks, IEEE 802.17 Resilient Packet Ring (RPR) [3–6]. The RPR standard aims at improving the throughput efficiency, service differentiation, and resilience of packet switched ring metropolitan area networks. Prestandard products have already been deployed in operational metro networks. An RPR is a bidirectional dual-fiber buffer insertion ring network that uses two performance-enhancing techniques: (i) destination stripping and (ii) shortest path routing. Unlike in source stripping, where the transmitting source node takes the packets from the ring, with destination stripping packets are removed from the ring by the receiving destination node. This allows nodes downstream of the destination node to spatially reuse bandwidth. As a consequence, more transmissions take place simultaneously, resulting in an improved network capacity. With shortest path routing, a given source node transmits data packets on that fiber which provides the shortest path to the corresponding destination node. Destination stripping in conjunction with shortest path routing improves the spatial reuse of bandwidth and thus the network capacity significantly.

Recently, research has begun to investigate the performance of the RPR standard and to propose performance improvements. It was shown in Refs. [7–9] that for unbalanced and constant-rate traffic inputs the RPR fairness control algorithm suffers from severe and permanent oscillations spanning nearly the entire range of the link capacity. Such oscillations hinder spatial reuse, decrease throughput, and increase delay jitter. The studied dynamic bandwidth allocation algorithms are able to mitigate the oscillations and achieve nearly complete spatial reuse.

In this paper we examine the performance of dual-fiber bidirectional buffer insertion rings as used in RPR for various traffic characteristics found in today's metro core and metro edge networks. RPR as a metropolitan ring network will be used in interconnected ring architectures, as typically deployed in metropolitan area networks. Metropolitan interconnected rings are composed of metro core and metro edge rings, where a metro core ring interconnects several metro edge rings, as shown in Fig. 1. Apart from inter-metro-edge-ring traffic, metro core rings also carry traffic from and to long-haul backbone networks. Metro edge rings in turn carry traffic between metro core rings and access networks, e.g., hybrid fiber coax, fiber-to-the-home, fiber-to-the-building networks, and passive optical networks. The traffic characteristics of metro core and metro edge rings are quite different. Metro edge rings exhibit strongly hubbed traffic, where most traffic originating from a given access network is outbound toward the metro core ring. In contrast, traffic demands in metro core rings are much more uniform, with any-to-any traffic between all attached nodes [10]. In this work we investigate the performance of dual-fiber bidirectional buffer insertion rings under typical traffic conditions and provide insight into their performance limitations. To mitigate these limitations and improve the performance of dual-fiber bidirectional buffer insertion rings, we introduce and examine a novel performance-enhancing technique that we call "proxy stripping." In brief, proxy stripping is used by ring nodes that are interconnected by an additional subnetwork that provides shortcuts to the peripheral ring network. Proxy stripping nodes pull packets from the ring and send them across the shortcuts of the subnetwork. As a result, the performance of dual-fiber bidirectional buffer

insertion rings is dramatically improved, in particular under hubbed (hot-spot) traffic as present in metro edge ring networks.
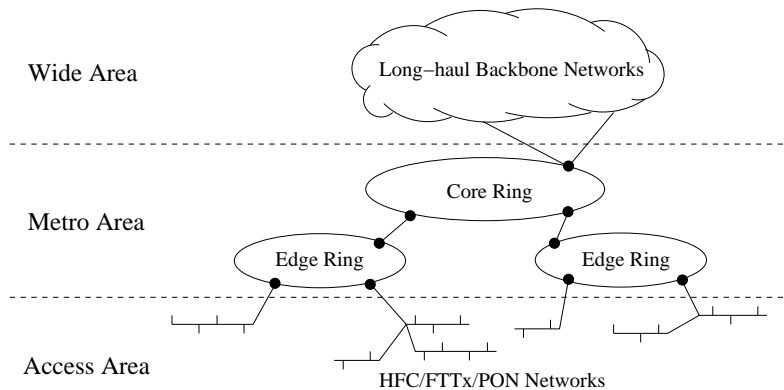

Fig. 1. Metro area networks: metro core rings interconnect metro edge rings and connect them to long-haul backbone networks.

The remainder of this paper is organized as follows. In the following paragraphs we review related work. Section 2 highlights the salient features of RPR. Section 3 describes the concept of proxy stripping in greater detail. In Section 4 we analyze the performance of dual-fiber bidirectional buffer insertion rings with and without proxy stripping for arbitrary traffic demands. In Section 5 we provide performance results obtained by the analysis and by verifying computer simulations. Section 6 concludes the paper.

Related Work. Augmented ring networks that deploy additional shortcut links to the ring in order to decrease the diameter and increase the bandwidth of the network have attracted considerable attention. For a graph-theoretical evaluation of various augmented ring networks the interested reader is referred to Ref. [11] and the references therein. In the area of wavelength division multiplexing (WDM) ring networks, so-called meshed rings achieve an increased spatial wavelength reuse factor by providing alternative paths in addition to the fiber rings [12, 13]. In meshed rings, multiple-wavelength routers are equally distributed among the ring nodes. Counter-directional pairs of fiber, so-called chords, are used to interconnect different pairs of wavelength routers. Augmenting ring networks with a star subnetwork has already been addressed to some extent previously. Bellcore's Star-Track switch is formed from two internal networks, a broadcast-and-select single-hop star WDM network based on optical passive star couplers (PSCs) and an electronic unidirectional token-based control ring [14, 15]. To access the star subnetwork, each node has one fixed-tuned transmitter and one tunable receiver. The control token ring is used for making reservations. After one ring round-trip propagation delay, data packets are sent across the star subnetwork. Star-Track does not allow for immediate ring access due to the token based protocol. A hybrid star-ring network based on multiple central wavelength routers in parallel was proposed in Ref. [16]. All ring nodes are connected to the central wavelength routers by either one or two pairs of fiber (so-called spokes). In addition, ring nodes are interconnected by a small number of fibers around the circumference carrying protection-switched traffic to standby spokes as well as residual working wavelength channels. The use of additional fibers in a ring around the periphery of the multiple-star network is one of the key features that allows total fiber quantities to be minimized. It was shown that, for a single-path failure and uniform traffic, fiber requirements are less than for a WDM add–drop multiplexer ring, while greater resilience to multiple-path failures is provided. The work focused primarily on path and wavelength router protection strategies and did not specify any medium access control (MAC) protocol. A multilevel star-ring architecture

consisting of a star network on the upper level and multiple concatenated ring subnets on the lower level was studied in Ref. [17]. The upper-level star network ensures high network capacity, and its weakness in reliability is overcome by the concatenated ring subnets with self-healing capabilities. The work concentrates on the physical transmission limitations rather than protocols. Again, a MAC protocol for such a modified star-ring architecture was not provided and investigated.

In this paper we evaluate the throughput-delay performance of a packet-switched dual-fiber bidirectional single-channel ring with and without proxy stripping. Our work differs from the aforementioned work as follows. As opposed to meshed rings, we do not use additional wavelength routers on the ring, and all proxy-stripping nodes are fully connected in a single-hop manner via the star subnetwork. In general, only a subset of the ring nodes are directly connected to the star network. The applied MAC protocol allows for immediate medium access on the ring. The integrated ring-star network forms a single-level architecture. We note that in a companion paper we have specified a star subnetwork based on an arrayed-waveguide grating (AWG), and we investigated the network performance for uniform traffic in terms of mean hop distance, spatial wavelength reuse, and capacity[18]. In this paper we investigate the throughput-delay performance of the proxy-stripping technique without specifying any particular star subnetwork. In our investigations we consider, apart from uniform traffic, also nonuniform symmetric and asymmetric traffic. The obtained results aim at assessing the maximum achievable throughput-delay performance of the proxy-stripping technique independent of any particular star subnetwork.

2. Resilient Packet Ring

As shown in Fig. 2, RPR is a bidirectional dual-fiber ring network with optical–electrical–optical (OEO) signal conversion at each of the N nodes [3–6]. Every node is equipped with two fixed-tuned transmitters (FTs) and two fixed-tuned receivers (FRs), one for each fiber ring. Broadcasting is achieved by means of source stripping. Each node has separate transit and station queues for either ring. Specifically, for each ring a node has one or two transit queues, one transmission queue termed a stage queue, one reception queue, and one add_MAC queue that stores control packets generated by the local node.
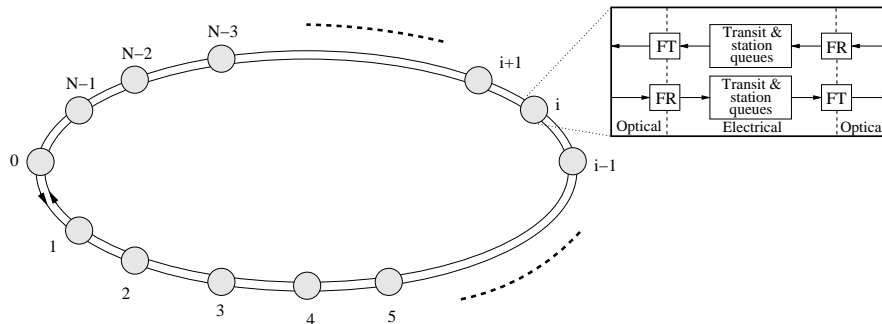

Fig. 2. Generic Resilient Packet Ring (RPR) network and node architecture connecting N nodes.

RPR nodes operate in one of two modes: (i) single-queue mode or (ii) dual-queue mode. In single-queue mode the transit path consists of a single FIFO queue termed the primary transit queue (PTQ). If the PTQ is not full, highest priority is given to add_MAC traffic. In absence of local control traffic, priority is given to in-transit ring traffic over station traffic. In dual-queue mode the transit path comprises two queues, one for guaranteed class A traffic (PTQ) and one secondary transit queue (STQ) for class B (committed rate) and

class C (best effort) traffic. In dual-queue mode, if both PTQ and STQ are not full, highest priority is given to add_MAC traffic (similar to single-queue mode). If there is no local control traffic, PTQ traffic is always served first. If the PTQ is empty, the local transmission queue (stage queue) is served until the STQ reaches a certain queue threshold. If the STQ reaches that threshold, STQ in-transit ring traffic is given priority over station traffic such that in-transit packets are not lost due to buffer overflow. Thus the transit path is lossless, and a packet put on the ring is not dropped at downstream nodes.

Furthermore, RPR defines fairness control algorithms that specify how a congested downstream node can throttle the transmission rate of upstream nodes by sending fairness control packets upstream. RPR provides a number of advantageous performance features. Among others, the counterrotating rings provide protection against any single link or node failure, and the dual-queue operation mode enables service differentiation, e.g., guaranteed QoS. Moreover, because of OEO conversion at each node, 3R signal regeneration (reamplifying, reshaping, retiming) can be provided in the electrical domain, which enables unamplified optical transmission between network nodes so that no expensive optical amplifiers are required.

3. Proxy Stripping

In RPR with destination stripping and shortest path routing the maximum hop distance is equal to $h_{\mathrm{max}} = \lceil (N-1)/2 \rceil$, whereby one hop denotes the distance between two adjacent nodes. Let the mean hop distance be equal to the average value of the minimum number of hops a data packet has to traverse on its shortest path from a given source node to all remaining $(N-1)$ destination nodes. Owing to the symmetry of the ring network, the mean hop distance is the same for all (source) nodes. For uniform traffic, i.e., if a given node sends a generated packet to any other node with equal probability $1/(N-1)$, the mean hop distance of RPR is given by

$$\overline{h} = \frac{2}{N-1} \sum_{j=1}^{\lfloor N-1/2 \rfloor} j + \frac{(N-1) \bmod 2}{N-1} \left\lceil \frac{N-1}{2} \right\rceil, \tag{1}$$

which reduces to

$$\overline{h} = \begin{cases} \frac{N+1}{4} & \text{if } N \text{ odd} \\ \frac{N^2/4}{N-1} & \text{if } N \text{ even} \end{cases}, \tag{2}$$

where $\lceil \bullet \rceil$ and $\lfloor \bullet \rfloor$ denote the ceiling function and the floor function, respectively. To see this relation, note that, since a given source node can send in both directions, two different destination nodes are reached up to a hop count of $\lfloor N-1/2 \rfloor$, which corresponds to the first term in Eq. (1). The second term in Eq. (1) accounts for the remaining (less than two) nodes, which are $\lceil N-1/2 \rceil$ hops away from the given source node. Note that for uniform traffic the mean hop distance equals approximately $N/4$ for each fiber ring. Hence, under uniform traffic up to four nodes can transmit on each ring simultaneously. As a result, in the bidirectional RPR network a total of up to eight nodes can transmit data simultaneously under uniform traffic.

To increase the capacity of RPR, we use dark (unlit) fibers to interconnect a subset of ring nodes in order to provide physical shortcuts. (Dark fibers are abundantly available in metropolitan regions, where public utility companies and new network operators make use of their right of ways to build and offer a fiber infrastructure that exceeds their current needs.) In doing so, data packets take the shortcuts instead of traveling along the ring, thereby consuming fewer bandwidth resources. As a consequence, packet transmissions are bounded to smaller ring segments, and more transmissions can take place on the ring simultaneously. Specifically, a subset of nodes P, $2 \le P \le N$, are attached to a central star

subnetwork by means of bidirectional dark fibers. The placement of the P nodes is done according to the given traffic demands. More precisely, nodes that generate and/or receive a large amount of traffic, e.g., hot-spot nodes, are best attached to the star subnetwork to benefit from the shortcuts of the star subnetwork. For uniform traffic where each node generates and receives the same amount of traffic, the P nodes are best equally spaced among the remaining ring nodes, as shown in Fig. 3 for $N = 12$ and $P = 4$. Thus, the placement of the P nodes may be different in metro edge and metro core networks, depending on the predominant type of traffic (hot-spot or uniform traffic). To guarantee minimum shortcuts in terms of hops, the star subnetwork is assumed to be a single-hop network, i.e., all P nodes are able to communicate with each other in one single hop without requiring any forwarding at intermediate nodes. The star subnetwork consists of dark fiber pairs, one per node, and a central hub. Proxy stripping is not restricted to any specific type of single-hop star network, node architecture, or MAC protocol. The hub of the star subnetwork can be either a wavelength-insensitive PSC or a wavelength-routing AWG. With a PSC, the star subnetwork forms a broadcast-and-select single-hop WDM star network, where each wavelength provides one communication channel. If more communication channels are required, e.g., due to a larger number of attached ring nodes P, the PSC can be replaced with an AWG. As opposed to the PSC, the AWG allows for spatial wavelength reuse; i.e., all wavelengths can be used at each AWG input port simultaneously without resulting channel collisions at the AWG output ports, leading to an increased number of communication channels. In both cases, access to the wavelengths of the star subnetwork is arbitrated by means of random, preallocation, or reservation MAC protocols. Unlike random and preallocation access protocols, reservation protocols use pretransmission coordination by sending a control packet prior to data transmission. Pretransmission coordination can be done by broadcasting high-priority control packets on either ring of RPR. It was shown in Ref. [4] that the latency of high-priority (control) traffic is constant and equal to the round-trip propagation delay of the ring, even under overload conditions. We note that the proposed proxy-stripping technique does not require any specific star subnetwork architecture, node architecture, or MAC protocol. Moreover, the star subnetwork does not necessarily have to operate at the same line rate as the peripheral RPR network, as we will see in Subsection 5.D. For more details on PSC-based single-hop star networks with different node structures and various MAC protocols, the interested reader is referred to Refs. [19] and [20]. Various AWG-based single-hop star network architectures in which each node is equipped with a single tunable transmitter and single tunable receiver or an array of fixed-tuned transceivers in conjunction with reservation access protocols are described in Ref. [21]. In an AWG-based star subnetwork in which each proxy-stripping node is equipped with an additional pair of tunable transmitter and tunable receiver, the mean hop distance, spatial reuse, and capacity of the resultant hybrid ring-star network was examined in Ref. [**?**].

To benefit from the shortcuts provided by the single-hop star subnetwork, each of the P nodes performs proxy stripping as well as source and destination stripping. With proxy stripping, each of the P nodes that is neither source nor destination pulls incoming data packets from the ring and sends them across the shortcuts to another proxy-stripping node that is either the destination of the data packets or closest to the corresponding destination node on the ring (by using the MAC protocol of the given single-hop star subnetwork). In the latter case the receiving proxy-stripping node forwards the data packets on the shortest path by choosing the appropriate ring. The destination node finally takes the data packets from the ring (destination stripping), as illustrated in Fig. 4 for source–destination pair A–C. Note that packets undergo proxy stripping only if the shortcuts provide a shorter path in terms of hops, where a hop denotes the distance between two adjacent nodes. Otherwise, data packets remain on the ring until they are received by the destination node, as shown in Fig. 4 for source–destination pair A–B. (Practically, this can be done by monitoring
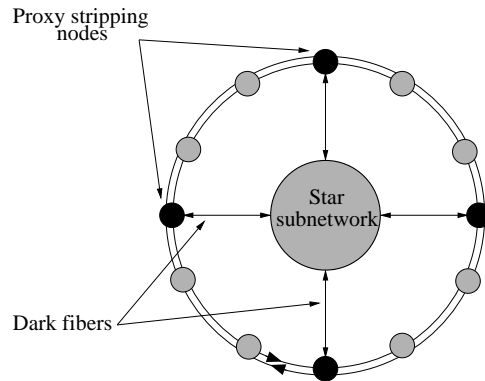
Fig. 3. RPR with $N = 12$ nodes, where $P = 4$ of them are interconnected by a dark-fiber single-hop star subnetwork.
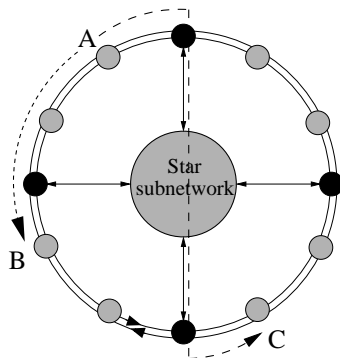

Fig. 4. Proxy stripping in conjunction with destination stripping and shortest path routing with source node A and destination nodes B and C.

each packet's source and destination MAC addresses and making a table lookup at proxy-stripping nodes with table entries indicating whether a given data packet has to be proxy stripped or not.)

To formally describe proxy stripping let us introduce the following variables for a given pair of source node s and destination node d, where $s, d \in \{0, 1, \ldots, N-1\}$:

- $h_{rs}(s)$, hop distance between the source node s and its closest proxy-stripping node.

- $h_{rs}(d)$, hop distance between the destination node d and its closest proxy-stripping node.

- $h_{\text{ring}}(s, d)$, minimum hop distance between the source node s and the destination node d on the ring, i.e., without proxy stripping.

- $h_{\text{star}}(s, d)$, minimum hop distance between the source node s and the destination node d via shortcuts of the single-hop star subnetwork, i.e., with proxy stripping. Note that $h_{\text{star}}(s, d) = h_{rs}(s) + 1 + h_{rs}(d)$.

Generally speaking, if the hop distance on the ring between a given source node s and destination node d is small enough, the source node sends the data packet(s) on the ring without undergoing proxy stripping. More precisely, if $h_{\text{ring}}(s, d) \leq h_{\text{star}}(s, d)$, then the source node s sends the data packet(s) to the destination node d along the ring on the shortest path by choosing the appropriate ring. The destination node d takes the transmitted data packet(s) from the ring (destination stripping). Note that in this case there is no proxy stripping (like node pair A–B in Fig. 4). Proxy stripping takes place only if $h_{\text{ring}}(s, d) > h_{\text{star}}(s, d)$, i.e., if the shortcuts form a shorter path between nodes s and d than either peripheral ring. Specifically, source node s sends the data packet(s) to its closest proxy-stripping node. Note that the chosen direction does not necessarily have to be the same as that in shortest path routing on the bidirectional ring. This implies that all ring nodes are aware of the presence and location of proxy-stripping nodes. As a consequence, packets travel along smaller ring segments, resulting in a decreased mean hop distance. (Alternatively, data packets could be sent in the same direction as in shortest path routing bidirectional rings. In doing so, we would obtain a larger mean hop distance. However, nodes would not need to have knowledge about the location of the P proxy-stripping nodes. Note that this would allow for a transparent proxy-stripping dark-fiber upgrade of RPR in which the remaining $(N-P)$ nodes do not have to be modified at all.) With proxy stripping, each of the P nodes takes the corresponding data packet(s) from the ring and sends the data packet(s) across the star subnetwork to the proxy-stripping node that is either the destination node or closest to the destination node. A given proxy-stripping node pulls only data packets from the ring whose source and destination addresses satisfy the condition $h_{\text{ring}}(s, d) > h_{\text{star}}(s, d)$. After transmitting a given data packet across the single-hop star subnetwork, the corresponding proxy-stripping node receives the packet and, if necessary, forwards it on the ring toward destination node d on the shortest path by using the appropriate ring. Destination node d finally takes the data packet from the ring (destination stripping). Beside proxy stripping and forwarding data packets, proxy-stripping nodes also generate traffic. Note that in this case $h_{rs}(s) = 0$. Again, if $h_{\text{ring}}(s, d) \leq h_{\text{star}}(s, d)$, then the proxy-stripping source node s transmits the data packet on that ring which provides the shortest path to destination node d. Otherwise, if $h_{\text{ring}}(s, d) > h_{\text{star}}(s, d)$, then the proxy-stripping source node s sends the data packet across the star subnetwork to the corresponding proxy-stripping node, which is either the destination itself or forwards the data packet onwards to node d via the shortest path ring.

Note that proxy stripping may be applied in both single-queue and dual-queue modes of RPR. In single-queue mode, proxy-stripped packets are put in an additional queue at

the corresponding proxy-stripping node for transmission across the star subnetwork. After traversing the star subnetwork, proxy-stripped packets are either received by the respective proxy-stripping node or, if necessary, are forwarded by putting them into the corresponding ring transit queue. In dual-queue mode, each proxy-stripping node has two additional queues for transmission across the star subnetwork. Proxy-stripped packets are put into one of these two queues according to their priority. After transmitting the proxy-stripped packets across the star subnetwork they are either received by the respective proxy-stripping node or, if necessary, are forwarded by putting them into the corresponding ring transit queue according to their priority. In doing so, proxy stripping preserves the priority of all packets. As for fairness, we note that each proxy-stripping node behaves like the regular ring nodes, i.e., executes the same fairness control algorithm like any regular ring node. Thus, the fair transmission and reception of packets on the bidirectional ring network is arbitrated by the RPR fairness control protocol. Fairness on the star subnetwork has to be provided by an appropriate protocol. For more details on a fair access protocol for the star subnetwork we refer the interested reader to Ref. [22].

Proxy stripping also improves the network resilience. In RPR, upon detection of a link or node failure the two ring nodes adjacent to the failed link or node switch all traffic arriving on the incoming fiber onto the outgoing fiber to reach the destination node going in the opposite direction. Thus the two ring nodes adjacent to the failure wrap all traffic away from the failed link or node. In the process wrapped traffic travels from the source node to the corresponding wrapping node, then back to the source node, and onward to the destination node along a secondary path, which in general is longer than the primary path in terms of hops, resulting in a rather inefficient use of bandwidth resources. With proxy stripping, wrapped traffic may be taken from the ring by the first encountered proxy-stripping node and sent across the star subnetwork to the proxy-stripping node closest to the destination node. As a result, with proxy stripping wrapped traffic makes use of the shortcuts of the star subnetwork and thus has to travel shorter backup paths, leading to a more efficient use of bandwidth resources. Furthermore, note that the star subnetwork divides the ring network into separate domains, each being fully recoverable from a single link or node failure without losing full network connectivity. As a consequence, the hybrid ring-star network is tolerant with respect to multiple failures, as opposed to the single-failure tolerance of RPR networks.

4. Analysis

In this section, we analyze the throughput-delay performance of the dual-fiber bidirectional ring both with and without proxy stripping. We note that in our analysis we do not take fairness control into account. The obtained results are intended to give the maximum achievable throughput-delay performance of RPR and to provide an upper bound that allows the performance of the various proposed fairness control protocols to be compared in order to see how far from the ideal they manage to perform.

4.A. Notation

Figure 5 depicts the bidirectional ring topology. The symbols $(+)$ and $(-)$ denote the clockwise and the counterclockwise directions of the ring, respectively. The number of ring nodes equals N, with P of them acting as proxy-stripping nodes, where $2 \leq P \leq N$. For simplicity we assume that the proxy-stripping nodes are equally spaced among the ring nodes at the position $i = 0, n, 2n, \ldots, N - n$, where $n = N/P$.
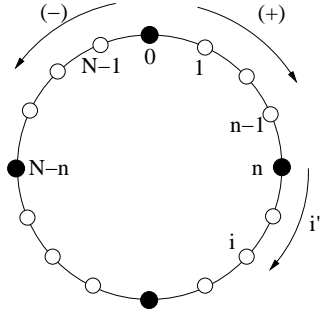
Fig. 5. Notation for ring direction and position of ring nodes.

Next, for a given node i, we define i' and i'' as follows:

$$i' = i \bmod N, \qquad (3)$$

$$i'' = i \bmod n, \qquad (4)$$

where i'' denotes the distance between a given node i and the closest proxy-stripping node in the $(-)$ direction, as shown in Fig. 5. The distance between a given node i and the closest proxy-stripping node in the $(+)$ direction is given by $n - i''$. The position of the proxy-stripping nodes in $(-)$ and $(+)$ directions next to node i equals $i - i''$ and $i - i'' + n$, respectively. The distance and position of both proxy-stripping nodes next to node i are summarized in Table 1.

Table 1. Distance and Position of Proxy Stripping Nodes Next to Node i

Direction	Distance to Next Proxy Node
$(-)$	i''
$(+)$	$N - i''$
$(-)$	$i - i''$
$(+)$	$i - i'' + N$

Let $f(i)$ denote the value of a given performance metric at node i, e.g., the waiting time an arriving data packet experiences in the transit queue of node i. To sum up the individual values of contiguous ring nodes, we introduce the following definition:

$$\sum_{i=a}^{b}{}^{*} f(i) := \begin{cases} \sum_{i=a'}^{b'} f(i) & \text{if } (a' \le b') \wedge (b' - a' \le \frac{N}{2}) \\ \sum_{i=a'}^{b'+N} f(i') & \text{if } (a' > b') \wedge (b' + N - a' \le \frac{N}{2}) \\ 0 & \text{else} \end{cases} \qquad (5)$$

Note that the above asterisked sum facilitates the notation by including the discontinuity at the transition from $i = N - 1$ to $i = 0$ in a convenient way. Otherwise, this transition would always have to be treated as a special case below. The asterisked sum equals 0 if the lower summation index is larger than the upper one, which is the case if the sum covers more than $N/2$ contiguous ring nodes. The double-asterisked sum does not have this restriction and is defined in this paper as

$$\sum_{i=a}^{b}{}^{**} f(i) := \begin{cases} \sum_{i=a'}^{b'} f(i) & \text{if } a' \le b' \\ \sum_{i=a'}^{b'+N} f(i') & \text{if } a' > b' \end{cases} \qquad (6)$$

4.B. Assumptions

In our analysis we make the following assumptions:

- *Single-queue mode*: We examine the single-queue mode of RPR; i.e., each node is equipped with one PTQ but no STQ. In addition, each node has a single transmit queue.

- *Infinite buffer size*: The size of both the PTQ and the transmit queue at each node is infinite. The infinite PTQ is well suited to model the lossless transit path of RPR.

- *Proxy stripping*: Packets that are proxy stripped from the ring are put into the star transmit queue of the corresponding proxy-stripping node. Packets that arrive from the star and need to be forwarded on the shortest path toward their destination are put into the corresponding transit queue of the receiving proxy-stripping node. As a result, proxy-stripped packets that need to be forwarded on the ring are processed like in-transit traffic and are thus given priority over locally generated station traffic. Thus the scheduling of proxy-stripped packets that need to be forwarded adheres to the scheduling algorithm of RPR in that priority is given to in-transit traffic over station traffic, as described in Section 2.

- *Propagation delay*: The nodes are equally spaced on the ring. The propagation delay between two adjacent ring nodes is given by τ. Thus, the round-trip time (RTT) of the RPR ring equals $N\tau$, which denotes the propagation delay from a given source node around the entire ring back to the same source node.

- *Unicast traffic*: We consider unicast traffic, i.e., all data transmissions are point-to-point.

- *Poisson packet arrival process*: The packet arrival process at the transmit queue of node i is Poisson with a mean arrival rate of $\lambda(i)$ packets per time unit, where $0 \leq i \leq N-1$. Note that the Poisson arrival rates of different nodes do not necessarily have to be the same.

- *Arbitrary packet length distribution*: We consider variable-size packets with an arbitrary packet length distribution, where $E[T_p]$ denotes the mean packet transmission time in time units.

- *Arbitrary traffic matrix*: A packet arriving at source node i is destined for node j with probability $p(i,j)$, where $0 \leq p(i,j) \leq 1$, $\sum_{j=0}^{N-1} p(i,j) = 1$, and $0 \leq i, j \leq N-1$. Thus, packets destined for node j arrive at the transmit queue of node i with a mean arrival rate of $\lambda(i,j) = \lambda(i)p(i,j)$. For each source–destination node pair (i,j) the amount of offered traffic is specified by the traffic matrix, whose elements are given by $\rho(i,j) = \lambda(i,j)E[T_p]$. Note that $\rho(i,j)$ measures the mean duration of arriving packets relative to the time unit. Thus, $\rho(i,j) = 1$ denotes the maximum packet arrival process with continuously newly arriving packets.

4.C. Performance Metrics

The performance of the networks is evaluated in terms of mean delay and mean aggregate throughput, which are defined as follows:

- *Mean Delay*: The mean delay denotes the average time period between packet arrival at the source node and packet reception at the destination node in steady state. The mean delay is given in time units.

- *Mean Aggregate Throughput*: The mean aggregate throughput denotes the mean number of transmitting nodes in steady state.

4.D. RPR with Proxy Stripping

The mean delay is equal to the weighted sum of the mean delay $d(i,j)$ of each source–destination node pair (i,j). The weights are the elements of the traffic matrix and represent the amount of traffic from source node i to destination node j. The mean delay d is given by

$$d = \frac{1}{\rho_{\text{tot}}} \sum_{i=0}^{N-1} \sum_{j=0}^{N-1} \rho(i,j) d(i,j), \tag{7}$$

with

$$\rho_{\text{tot}} = \sum_{i=0}^{N-1} \sum_{j=0}^{N-1} \rho(i,j). \tag{8}$$

Depending on whether proxy stripping occurs or not, the mean delay of source–destination node pair (i,j) is obtained as

$$d(i,j) = \begin{cases} d_{\text{ring}}(i,j) & \text{if } h_{\text{ring}}(i,j) \leq h_{rs}(i) + 1 + h_{rs}(j) \\ d_{rs}(i) + d_{\text{star}} + d_{sr}(j) & \text{else} \end{cases}, \tag{9}$$

where

$$h_{\text{ring}}(i,j) = \min\{|i-j|, N-|i-j|\}, \tag{10}$$

$$h_{rs}(l) = \min\{l'', n-l''\}, \quad l \in \{i,j\}. \tag{11}$$

To see this, recall from Section 3 that proxy stripping does not take place if the path on the peripheral ring is shorter than or equal to that using the shortcuts of the star subnetwork in terms of hops, i.e., $h_{\text{ring}}(i,j) \leq h_{rs}(i) + 1 + h_{rs}(j)$. Otherwise, packets undergo proxy stripping. The hop distance between a given node i and the two neighboring proxy-stripping nodes and the hop distance between source node i and destination node j on the ring are illustrated in Fig. 6. These distances are used to determine $h_{\text{ring}}(i,j)$ and $h_{rs}(l)$ in Eqs. (10) and (11), respectively. As illustrated in Fig. 7, without proxy stripping $d(i,j)$ equals $d_{\text{ring}}(i,j)$, which denotes the mean delay encountered on the shortest ring path between source node i and destination node j. With proxy stripping, $d(i,j)$ equals $d_{rs}(i) + d_{\text{star}} + d_{sr}(j)$, where $d_{rs}(i)$ denotes the mean delay encountered between source node i and its closest proxy-stripping node, d_{star} denotes the time period required for transmitting the corresponding proxy-stripped packet across the star subnetwork, and $d_{rs}(j)$ denotes the mean delay encountered between destination node j and its closest proxy-stripping node. Next, we need to calculate $d_{\text{ring}}(i,j)$, $d_{rs}(i)$, $d_{rs}(j)$, and d_{star}.
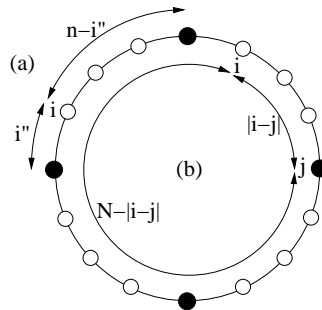

Fig. 6. Hop distances (a) between node i and neighboring proxy-stripping nodes and (b) between source node i and destination node j (in both directions).
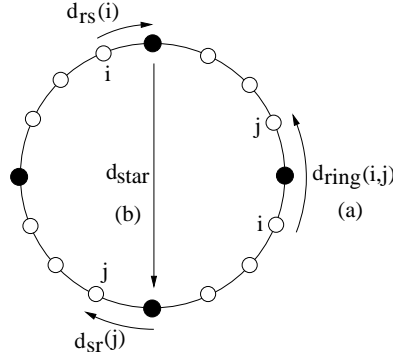
Fig. 7. Mean delay of source-destination node pair (i, j) (a) without proxy stripping and (b) with proxy stripping.

The mean delay $d_{\mathrm{ring}}(i, j)$ for a ring-only transmission without proxy stripping is composed of the mean waiting time $w_t(i)$ encountered at the transmit queue of source node i, the mean packet transmission time $E[T_p]$, the link propagation delay τ, and the mean waiting time $w_r(k)$ encountered at the transit queues of nodes k between source node i and destination node j. The mean delay $d_{\mathrm{ring}}(i, j)$ is given by

$$d_{\mathrm{ring}}(i, j) = \begin{cases} d_{\mathrm{ring}}^+(i, j) & \text{if } \left[(i < j) \wedge \left(j - i < \frac{N}{2}\right)\right] \vee \left[(i > j) \wedge \left(i - j > \frac{N}{2}\right)\right] \\ d_{\mathrm{ring}}^-(i, j) & \text{if } \left[(i < j) \wedge \left(j - i > \frac{N}{2}\right)\right] \vee \left[(i > j) \wedge \left(i - j < \frac{N}{2}\right)\right] \\ \frac{1}{2}d_{\mathrm{ring}}^+(i, j) + \frac{1}{2}d_{\mathrm{ring}}^-(i, j) & \text{if } |i - j| = N/2 \\ 0 & \text{if } (i = j) \end{cases},$$

(12)

with

$$d_{\mathrm{ring}}^+(i, j) = w_t^+(i) + E[T_p] + \tau + \sum_{k=i+1}^{j-1}{}^* \left(w_r^+(k) + \tau\right),$$

(13)

$$d_{\mathrm{ring}}^-(i, j) = w_t^-(i) + E[T_p] + \sum_{k=j+1}^{i-1}{}^* \left(w_r^-(k) + \tau\right).$$

(14)

As depicted in Fig. 8, two different cases have to be considered for either direction, which is indicated by the upper indices $(+)$ and $(-)$. In Eq. (12), the first and second line of the first "if" correspond to (a) and (b) in the figure, and the first and second line of the second "if" correspond to (c) and (d) in the figure (the third and fourth "if" are not illustrated in the figure).

Similarly, the mean delay $d_{rs}(i)$ is given by

$$d_{rs}(i) = \begin{cases} d_{rs}^-(i) & \text{if } 0 < i'' < \frac{n}{2} \\ d_{rs}^+(i) & \text{if } i'' > \frac{n}{2} \\ \frac{1}{2}d_{rs}^-(i) + \frac{1}{2}d_{rs}^+(i) & \text{if } i'' = \frac{n}{2} \\ 0 & \text{if } i'' = 0 \end{cases},$$

(15)

with

$$d_{rs}^-(i) = w_t^-(i) + E[T_p] + \tau + \sum_{k=i-i''+1}^{i-1} \left(w_r^-(k) + \tau\right),$$

(16)

$$d_{rs}^+(i) = w_t^+(i) + E[T_p] + \tau + \sum_{k=i+1}^{i-i''+n-1} \left(w_r^+(k) + \tau\right).$$
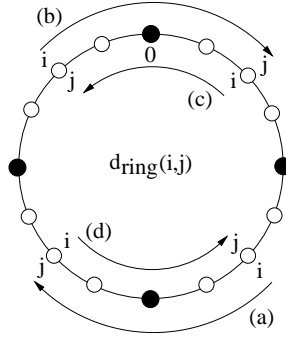
(17)

Fig. 8. Mean delay $d_{\text{ring}}(i,j)$ of a ring-only transmission without proxy stripping between source node i and destination node j.

Note that if n is even, the number of regular ring nodes between two neighboring proxy-stripping nodes is odd. Thus, for even n one regular ring node between two neighboring proxy-stripping nodes has the same hop distance to both proxy-stripping nodes, namely $n/2$. In this case, nodes in the middle split their traffic equally and transmit the same amount of traffic in both directions, resulting in improved load balancing. Reordering of the packets at the destination node is done by higher-level protocols. (Alternatively, packets could be transmitted only in one direction according to a given arbitration rule.)

Packets arriving from the star are put in the transit queue of the receiving proxy-stripping node and are forwarded toward their destination node j. The forwarded packets traverse all transit queues of the intermediate nodes between the corresponding proxy-stripping node and destination node j. Accordingly, the mean delay $d_{sr}(j)$ is given by

$$
d_{sr}(j) = \begin{cases} d_{sr}^+(j) & \text{if } 0 < j'' < \frac{n}{2} \\ d_{sr}^-(j) & \text{if } j'' > \frac{n}{2} \\ \frac{1}{2}d_{sr}^+(j) + \frac{1}{2}d_{sr}^-(j) & \text{if } j'' = \frac{n}{2} \\ 0 & \text{if } j'' = 0 \end{cases}, \tag{18}
$$

with

$$
d_{sr}^+(j) = \sum_{k=j-j''}^{j-1} \left(w_r^+(k) + \tau \right), \tag{19}
$$

$$
d_{sr}^-(j) = \sum_{k=j+1}^{j-j''+n} \left(w_r^-(k) + \tau \right). \tag{20}
$$

The mean delay d_{star} depends on the access control used in the star subnetwork. For random and preallocation access control d_{star} is given by

$$
d_{\text{star}} = E\left[T_p^{\text{star}} \right] + \frac{N\tau}{\pi}, \tag{21}
$$

where $E\left[T_p^{\text{star}} \right]$ denotes the mean packet transmission time on the star subnetwork and $N\tau/\pi$ denotes the propagation delay of the star subnetwork. For reservation access control with pretransmission coordination via the ring d_{star} is given by

$$
d_{\text{star}} = N\tau + E\left[T_p^{\text{star}} \right] + \frac{N\tau}{\pi}, \tag{22}
$$

where $N\tau$ represents the RTT of the ring. Note that in Eqs. (21) and (22) we assume that the star subnetwork provides sufficient capacity such that the waiting time at the star transmit

queues of the proxy-stripping nodes is negligible. This assumption is motivated by the fact that in this work we aim at demonstrating the potential of the proxy-stripping technique rather than addressing the design of a specific star subnetwork. (For a more detailed analysis of capacity-constrained star subnetworks that take nonzero waiting times at the star transmit queues of proxy-stripping nodes into account, we refer the interested reader to Appendix A of this paper.)

Next, for the above expressions of $d_{\mathrm{ring}}(i,j)$, $d_{rs}(i)$, and $d_{sr}(j)$ we need to calculate the mean waiting time in the transmit queue $w_t^{\pm}(i)$ and the mean waiting time in the transit queue $w_r^{\pm}(i)$ at node i. Under the assumption that the packet arrival process at the transit queue is Poisson, the mean waiting times in both the transmit queue and transit queue were analyzed in Ref. [18] for the case of unidirectional rings. By extending these results to our bidirectional ring we obtain $w_t^{\pm}(i)$ as

$$w_t^{\pm}(i) = \frac{\left(\rho_r^{\pm}(i) + \rho_t^{\pm}(i)\right) E\left[T_p^2\right]}{2\left(1 - \rho_r^{\pm}(i) - \rho_t^{\pm}(i)\right)\left(1 - \rho_r^{\pm}(i)\right) E\left[T_p\right]} \tag{23}$$

and $w_r^{\pm}(i)$ as

$$w_r^{\pm}(i) = \frac{\rho_t^{\pm}(i) E\left[T_p^2\right]}{2\left(1 - \rho_r^{\pm}(i)\right) E\left[T_p\right]}, \tag{24}$$

where $\rho_t^{\pm}(i)$ and $\rho_r^{\pm}(i)$ denote the amount of traffic arriving at the ring transmit queues and the ring transit queues of both directions $(+)$ and $(-)$ at node i, respectively (to be defined shortly). In Section 5 we show by means of extensive verifying simulations that our analysis provides very accurate results despite the simplifying assumption of Poisson arrivals at transit queues. Next, we calculate the amount of traffic arriving at the ring transmit queues $\rho_t^{\pm}(i)$ and the ring transit queues $\rho_r^{\pm}(i)$ at node i for both directions $(+)$ and $(-)$.

4.D.1. Ring Transmit Queues

The amount of traffic $\rho_t^{\pm}(i)$ that arrives at the ring transmit queue of node i and corresponds to the direction toward the closest proxy-stripping node is composed of the ring-only traffic $\rho_t^{r\pm}(i)$ for that direction and all traffic $\rho_t^{\mathrm{out}}(i)$ that is sent via the star subnetwork. For the other direction, $\rho_t^{\pm}(i)$ comprises the ring-only traffic for that direction. If n is even and the node i is located between two adjacent proxy-stripping nodes, i.e., $i'' = n/2$, the star traffic is equally split and sent in both directions. The total amount of traffic originating from node i equals $\rho_t^{\pm}(i) = \rho_t^{+}(i) + \rho_t^{-}(i)$, where $\rho_t^{+}(i)$ and $\rho_t^{-}(i)$ are given by

$$\rho_t^{+}(i) = \begin{cases} \rho_t^{r+}(i) & \text{if } 0 \leq i'' < n - i'' \\ \rho_t^{r+}(i) + \frac{1}{2}\rho_t^{\mathrm{out}}(i) & \text{if } i'' = n - i'' \\ \rho_t^{r+}(i) + \rho_t^{\mathrm{out}}(i) & \text{if } i'' > n - i'' \end{cases}, \tag{25}$$

$$\rho_t^{-}(i) = \begin{cases} \rho_t^{r-}(i) & \text{if } \left(i'' = 0\right) \vee \left(i'' > n - i''\right) \\ \rho_t^{r-}(i) + \frac{1}{2}\rho_t^{\mathrm{out}}(i) & \text{if } i'' = n - i'' \\ \rho_t^{r-}(i) + \rho_t^{\mathrm{out}}(i) & \text{if } 0 < i'' < n - i'' \end{cases}. \tag{26}$$

As depicted in Fig. 9, source node i sends packets directly on the ring without proxy stripping up to destination node $r^{-}(i)$ in the $(-)$ direction and up to destination node $r^{+}(i)$ in the $(+)$ direction. The remaining destination nodes are reached by means of proxy stripping. The nodes $r^{\pm}(i)$ are given by

$$r^{+}(i) = \begin{cases} i + \left\lceil \frac{n}{2} \right\rceil & \text{if } i'' < \left\lfloor \frac{n}{2} \right\rfloor \\ i + n & \text{if } i'' = \left\lfloor \frac{n}{2} \right\rfloor \\ i - i'' + n + \left\lceil \frac{n}{2} \right\rceil & \text{if } i'' > \left\lfloor \frac{n}{2} \right\rfloor \end{cases}, \tag{27}$$

$$r^-(i) = \begin{cases} i - i'' - \lceil \frac{n}{2} \rceil & \text{if } i'' < \lceil \frac{n}{2} \rceil \\ i - n & \text{if } i'' = \lceil \frac{n}{2} \rceil \\ i - \lceil \frac{n}{2} \rceil & \text{if } i'' > \lceil \frac{n}{2} \rceil \end{cases} . \tag{28}$$
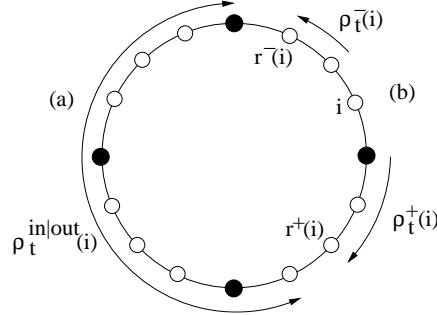

Fig. 9. Destination nodes reached by source node i (a) with proxy stripping and (b) without proxy stripping.

Figure 10 shows the three different cases in the calculation of $r^\pm(i)$. In Eqs. (27) and (28) the first "if" corresponds to (a), the second to (b), and the third to (c) in the figure. Given $r^\pm(i)$, we obtain $\rho_t^{r+}(i)$, $\rho_t^{r-}(i)$, and $\rho_t^{\text{out}}(i)$ as

$$\rho_t^{r+}(i) = \sum_{j=i+1}^{r^+(i)} {}^* \rho(i,j) - \begin{cases} \frac{1}{2}\rho(i,r^+(i)) & \text{if } |i - r^+(i)| = N/2 \\ 0 \end{cases}, \tag{29}$$

$$\rho_t^{r-}(i) = \sum_{j=r^-(i)}^{i-1} {}^* \rho(i,j) - \begin{cases} \frac{1}{2}\rho(i,r^-(i)) & \text{if } |i - r^-(i)| = N/2 \\ 0 & \text{else} \end{cases}, \tag{30}$$

$$\rho_t^{\text{out}}(i) = \begin{cases} 0 & \text{if } \left(n = \frac{N}{2}\right) \wedge \left[\left(i'' = \lfloor \frac{n}{2} \rfloor\right) \vee \left(i'' = \lceil \frac{n}{2} \rceil\right)\right] \\ \sum_{j=r^+(i)+1}^{r^-(i)-1} {}^{**} \rho(i,j) & \text{else} \end{cases} . \tag{31}$$
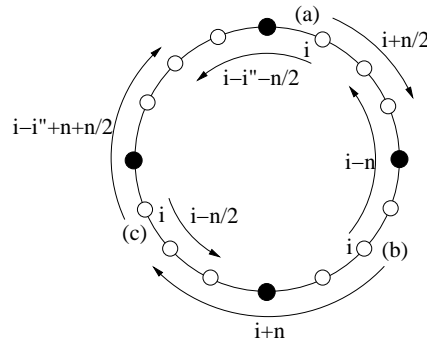

Fig. 10. Ring segments that are reached by source node i without proxy stripping.

4.D.2. Ring Transit Queues

The amount of traffic $\rho_r^{\pm}(i)$ that arrives at the ring transit queue of node i is composed of the forwarded ring-only traffic $\rho_r^{r\pm}(i)$ and the traffic $\rho_r^{s\pm}(i)$ forwarded either from or to the star, depending on the position of node i. Hence, $\rho_r^{\pm}(i)$ is given by

$$\rho_r^{\pm}(i) = \rho_r^{r\pm}(i) + \rho_r^{s\pm}(i). \tag{32}$$

As illustrated on the right-hand side of Fig. 11, the forwarded ring-only traffic $\rho_r^{r\pm}(i)$ is composed of the traffic that originates from the nodes before node i and is destined to nodes behind node i. In the figure, each arrow corresponds to a different node before node i and covers the nodes behind node i. Thus, for each direction $\rho_r^{r\pm}(i)$ is given by

$$\rho_r^{r+}(i) = \sum_{k=r^-(i)}^{i-1}{}^* \left(\sum_{l=i+1}^{r^+(k)}{}^* \rho(k,l) - \begin{cases} \frac{1}{2}\rho(k,r^+(k)) & \text{if } |k - r^+(k)| = N/2 \\ 0 & \end{cases} \right), \tag{33}$$

$$\rho_r^{r-}(i) = \sum_{k=i+1}^{r^+(i)}{}^* \left(\sum_{l=r^-(k)}^{i-1}{}^* \rho(k,l) - \begin{cases} \frac{1}{2}\rho(k,r^-(k)) & \text{if } |k - r^-(k)| = N/2 \\ 0 & \end{cases} \right). \tag{34}$$
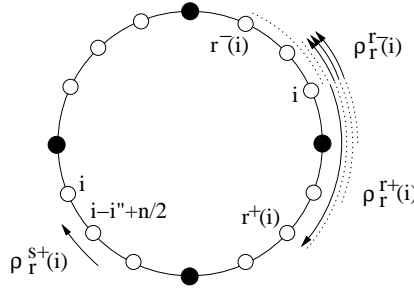

Fig. 11. Illustration of forwarded ring-only traffic.

Similarly, the traffic $\rho_r^{s\pm}(i)$ forwarded from (or to) the star is composed of the aggregate traffic $\rho_t^{in}(k)$ [or $\rho_t^{out}(k)$ of Eq. (31)] of all nodes between the closest proxy-stripping node before and all nodes behind node i, where $\rho_t^{in}(k)$ is given by

$$\rho_t^{in}(k) = \begin{cases} 0 & \text{if } \left(n = \frac{N}{2}\right) \wedge \left[\left(k'' = \lfloor\frac{n}{2}\rfloor\right) \vee \left(k'' = \lceil\frac{n}{2}\rceil\right)\right] \\ \sum_{j=r^+(k)+1}^{**r^-(k)-1} \rho(j,k) & \text{else} \end{cases}. \tag{35}$$

For each direction $\rho_r^{s\pm}(i)$ is given by

$$\rho_r^{s+}(i) = \begin{cases} \sum_{k=i+1}^{i-i''+\lfloor n/2\rfloor} \rho_t^{in}(k) & - \begin{cases} \frac{1}{2}\rho_t^{in}\left(i-i''+\frac{n}{2}\right) & \text{if } n \text{ even} \\ 0 & \text{if } n \text{ odd} \end{cases} & \text{if } 0 \le i'' < \lfloor\frac{n}{2}\rfloor \\ \sum_{k=i-i''+\lceil n/2\rceil}^{i-1} \rho_t^{out}(k) & - \begin{cases} \frac{1}{2}\rho_t^{out}\left(i-i''+\frac{N}{2}\right) & \text{if } n \text{ even} \\ 0 & \text{if } n \text{ odd} \end{cases} & \text{if } i'' > \lceil\frac{n}{2}\rceil \\ 0 & \text{if } \left(i'' = \lfloor\frac{n}{2}\rfloor\right) \vee \left(i'' = \lceil\frac{n}{2}\rceil\right) \end{cases}, \tag{36}$$

$$\rho_r^{s-}(i) = \begin{cases} \sum_{k=i+1}^{i-i''+\lfloor n/2 \rfloor} \rho_t^{\text{out}}(k) & - \begin{cases} \frac{1}{2}\rho_t^{\text{out}}\left(i-i''+\frac{n}{2}\right) & \text{if } n \text{ even} \\ 0 & \text{if } n \text{ odd} \end{cases} & \text{if } 0 < i'' < \lfloor \frac{n}{2} \rfloor \\[3ex] \sum_{k=i-i''+\lceil n/2 \rceil}^{i-1} \rho_t^{\text{in}}(k) & - \begin{cases} \frac{1}{2}\rho_t^{\text{in}}\left(i-i''+\frac{N}{2}\right) & \text{if } n \text{ even} \\ 0 & \text{if } n \text{ odd} \end{cases} & \text{if } \left(i''=0\right) \vee \left(i'' > \lceil \frac{n}{2} \rceil\right) \\[3ex] 0 & \text{if } \left(i'' = \lfloor \frac{n}{2} \rfloor\right) \vee \left(i'' = \lceil \frac{n}{2} \rceil\right) \end{cases} \tag{37}$$

Note that proxy-stripping nodes and nodes located in the middle of adjacent proxy-stripping nodes do not forward any star traffic.

4.D.3. Star Transmit Queues

To evaluate the forwarding burden caused by proxy stripping, we also calculate the amount of traffic arriving at proxy-stripping nodes. The amount of traffic $\rho_s(i)$ that arrives at the star transmit queue of node i, $i = 0, n, 2n, \ldots, (N-n)$, consists of the traffic to be stripped from both rings and the traffic generated and sent by the proxy-stripping node itself via the star subnetwork. Thus, $\rho_s(i)$ is given by

$$\rho_s(i) = \rho_r^{s+}\left((i-1)'\right) + \rho_t^{\text{out}}\left((i-1)'\right) + \rho_t^{\text{out}}(i) + \rho_t^{\text{out}}(i+1) + \rho_r^{s-}(i+1), \tag{38}$$

where ρ_t^{out}, ρ_r^{s+}, and ρ_r^{s-} are given in Eqs. (31), (36), and (37), respectively.

4.E. RPR Without Proxy Stripping

In this section, we analyze the throughput-delay performance of RPR without proxy stripping. As opposed to the above analysis, in RPR without proxy stripping there is no star subnetwork and the above equations are modified as follows. Equation (9) reduces to $d(i,j) = d_{\text{ring}}(i,j)$ and Eq. (7) becomes

$$d = \frac{1}{\rho_{\text{tot}}} \sum_{i=0}^{N-1} \sum_{j=0}^{N-1} \rho(i,j) d_{\text{ring}}(i,j). \tag{39}$$

The expressions for the waiting times $w_t^{\pm}(i)$ and $w_r^{\pm}(i)$ of Eqs. (23) and (24) also hold for RPR without proxy stripping. However, the calculation of $\rho_t^{\pm}(i)$ and $\rho_r^{\pm}(i)$ is different, since in RPR without proxy stripping there is no star subnetwork. For the ring transmit queues, Eqs. (25) and (26) reduce to $\rho_t^+(i) = \rho_t^{r+}(i)$ and $\rho_t^-(i) = \rho_t^{r-}(i)$, respectively. Furthermore, Eqs. (29) and (30) have to be slightly modified as follows:

$$\rho_t^{r+}(i) = \sum_{j=i+1}^{r^+(i)*} \rho(i,j) - \begin{cases} \frac{1}{2}\rho(i,r^+(i)) & \text{if } N \text{ even} \\ 0 & \text{if } N \text{ odd} \end{cases}, \tag{40}$$

$$\rho_t^{r-}(i) = \sum_{j=r^-(i)}^{i-1*} \rho(i,j) - \begin{cases} \frac{1}{2}\rho(i,r^-(i)) & \text{if } N \text{ even} \\ 0 & \text{if } N \text{ odd,} \end{cases}, \tag{41}$$

where $r^+(i)$ and $r^-(i)$ are given by

$$r^+(i) = i + \lfloor N/2 \rfloor, \tag{42}$$

$$r^-(i) = i - \lfloor N/2 \rfloor. \tag{43}$$

Note that without proxy stripping all nodes are reached via the ring. Consequently, the borders of ring-only transmissions $r^{\pm}(i)$ cover the whole ring now. Each direction covers one half of the ring corresponding to shortest path routing and traffic from source node i destined for the opposite ring node is equally split and sent in both directions. Similarly, for the ring transit queues Eq. (32) reduces to $\rho_r^{\pm}(i) = \rho_r^{r\pm}(i)$. In addition, Eqs. (33) and (34) are modified as follows

$$\rho_r^{r+}(i) = \sum_{k=r^-(i)+1}^{i-1} \left(\sum_{l=i+1}^{r^+(k)} \rho(k,l) - \left\{ \begin{array}{ll} \frac{1}{2}\rho(j,r^+(k)) & \text{if } N \text{ even} \\ 0 & \text{if } N \text{ odd} \end{array} \right. \right), \qquad (44)$$

$$\rho_r^{r-}(i) = \sum_{k=i+1}^{r^+(i)-1} \left(\sum_{l=r^-(k)}^{i-1} \rho(k,l) - \left\{ \begin{array}{ll} \frac{1}{2}\rho(j,r^-(k)) & \text{if } N \text{ even} \\ 0 & \text{if } N \text{ odd} \end{array} \right. \right). \qquad (45)$$

5. Results

In this section, we conduct numerical investigations of the throughput-delay performance of RPR both with and without proxy stripping for different traffic matrices. The default network parameters are set as follows: the line rate of each ring equals 2.5 Gb/s, the signal propagation delay equals $\frac{2}{3}c_o$, where $c_o = 3 \times 10^8$ m/s, and the circumference of the bidirectional ring equals $l = 100$ km, i.e., the RTT of the ring is constant and equals $N\tau = 3l/2c_o$. The line rate of each dark fiber is assumed to be equal to 10 Gb/s. For the packet size we use the trimodal distribution that is typically found in IP networks, as shown in Table 2. (We note that the emergence of new applications, e.g., content distribution networks and media streaming, may result in different packet length distributions on specific links. However, on a large number of links the typical trimodal packet length distribution is still valid [24].) Without loss of generality, we set $E\left[T_p^{\text{star}}\right] = 0$. To verify the accuracy of our analytical model, we have also conducted extensive simulations. In each simulation we have generated 10^6 packets including a warm-up phase of 10^5 packets. Using the method of batch means we calculated the 95% confidence intervals for the performance metrics. As opposed to the analysis, in our simulations we do not assume Poisson packet arrivals at the transit queue of each node.

Table 2. Trimodal Packet Length Distribution

Length (bytes)	Portion of Packets (%)
40	50
552	30
1500	20

In the following, we examine the throughput-delay performance of RPR and its limitations under uniform, hot-spot, and asymmetric traffic. We thereby pay particular attention to the effect of proxy stripping on the performance of RPR.

5.A. Uniform Traffic

Under uniform traffic a given node sends a generated packet to any other node with equal probability $1/(N-1)$. Recall from Section 1 that uniform traffic is typically found in metro core rings. Figures 12 and 13 depict the mean delay (given in multiples of the ring RTT) versus mean aggregate throughput (number of simultaneously transmitting nodes) both without and with proxy stripping for different numbers of nodes $N \in \{8, 16, 256\}$. As is shown in Fig. 12, without proxy stripping the mean delay is equal to one fourth of the RTT for

light loads, since for uniform traffic packets traverse one fourth of the ring on average without experiencing any significant queueing delay. For an increasing offered load the channel utilization increases until all bandwidth resources are fully utilized. Under high channel utilization, nodes have to wait for a longer time period to find the channel idle, resulting in an increased delay. The maximum mean aggregate throughput of RPR is given by the ratio of the number of links divided by the mean hop distance $2N/\bar{h}$, where $\bar{h}$ is given in Eq. (2) of Section 3. We observe from Fig. 12 that RPR achieves a maximum mean aggregate throughput of seven to eight, depending on N. Note that for small N the analytical and simulative results match perfectly, while for an increasing N the simulation provides a slightly larger throughput. This is because we assumed Poisson packet arrivals at the transit queue of each node. With increasing N the error caused by this simplifying assumption is accumulated, resulting in a more pronounced discrepancy between analysis and simulation, where the analysis slightly underestimates the more realistic simulation results.

Figure 13 shows the effect of proxy stripping on the throughput-delay performance of RPR using $P \in \{2,4\}$ proxy-stripping nodes. (The three leftmost curves are for $P = 2$, the three rightmost curves are for $P = 4$.) Interestingly, using $P = 2$ proxy-stripping nodes increases the maximum mean aggregate throughput of RPR only for $N = 8$. In contrast, for $N = 16$ and in particular $N = 256$, using $P = 2$ proxy-stripping nodes slightly deteriorates the throughput-delay performance of RPR. This is because with proxy stripping source ring nodes send some of their packets to the closest proxy-stripping nodes rather than directly to the corresponding destination nodes. As a consequence, the proxy-stripping nodes form a hot spot whose attached ring fibers become more congested with increasing traffic load. These congested fiber links prevent ring nodes from sending more data packets, resulting in a decreased throughput and a slightly increased delay. Clearly, with increasing N and $P = 2$ fixed the congestion becomes more severe. The congestion on the fiber links close to the proxy-stripping nodes can be mitigated by increasing the number of proxy-stripping nodes, as depicted in Fig. 13 for $P = 4$. We observe that the throughput of RPR using $P = 4$ proxy-stripping nodes is better than that of RPR without proxy stripping for all $N \in \{8, 16, 256\}$. Note that in Fig. 13 analysis and simulation results match very well. This is because with proxy-stripping data packets are sent via the shortcuts of the star subnetwork and thus traverse fewer ring transit queues on average. Consequently, the error due to the assumed Poisson arrival at transit queues in the analysis is less pronounced.

Figure 14 shows the throughput-delay performance of RPR for different numbers of proxy-stripping nodes $P \in \{4, 8, 16, 32, 64\}$ and $N = 256$ fixed. Obviously, the throughput of RPR is dramatically improved by increasing P. For instance, by interconnecting $32/256 = 12.5\%$ of the nodes via a star subnetwork, i.e., $P = 32$, a maximum mean aggregate throughput of approximately 75 is achieved. Compared with Fig. 12, this translates into a throughput improvement by a factor of almost ten. As is shown in Fig. 14, the throughput performance of RPR can be further improved by increasing P at the expense of more star transceivers and dark fibers. Note that at light loads the mean delay is slightly larger than one fourth of RTT. This is due to the queueing delays encountered at the ring transit queues of the hot-spot proxy-stripping nodes.

So far, we have considered star subnetworks without pretransmission coordination overhead, e.g., preallocation and random access protocols. That is, the transmission of proxy-stripped packets across the shortcuts of the star subnetwork did not imply any reservation overhead. Figure 15 depicts the throughput-delay performance of RPR if channel access on the star subnetwork is arbitrated by a reservation protocol with pretransmission coordination for $P \in \{4, 8, 16, 32, 64\}$ and $N = 256$. Recall from Subsection 4.D that with pretransmission coordination control packets are broadcast along either ring prior to data transmission, resulting in an overhead of $N\tau$ time units (RTT). Consequently, the throughput-delay curves are shifted toward higher delay values, as depicted in Fig. 15. We observe from the
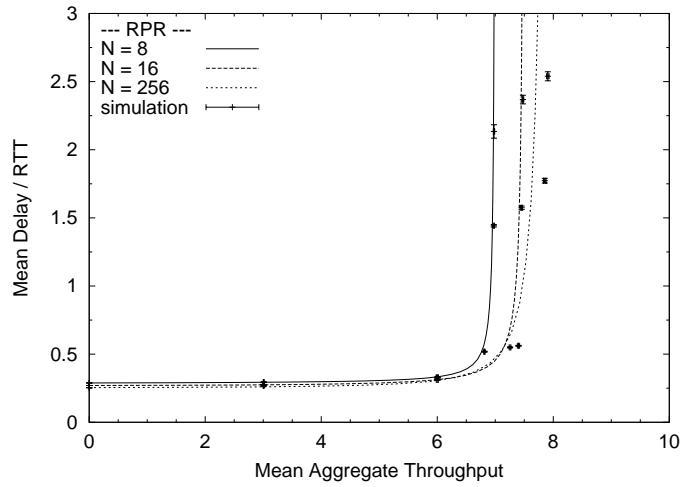
Fig. 12. Mean delay versus mean aggregate throughput of RPR without proxy stripping for uniform traffic with different $N \in \{8, 16, 256\}$.
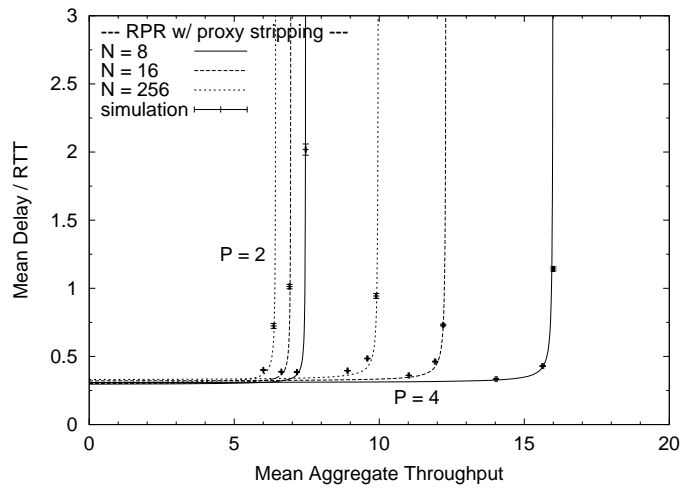

Fig. 13. Mean delay versus mean aggregate throughput of RPR with $P \in \{2, 4\}$ proxy-stripping nodes for uniform traffic with different $N \in \{8, 16, 256\}$.
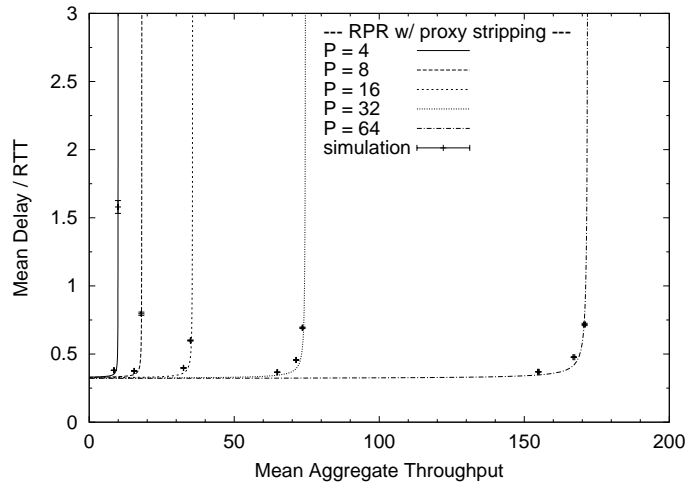
Fig. 14. Mean delay versus mean aggregate throughput of RPR with $P \in \{4, 8, 16, 32, 64\}$ proxy-stripping nodes for uniform traffic with $N = 256$.
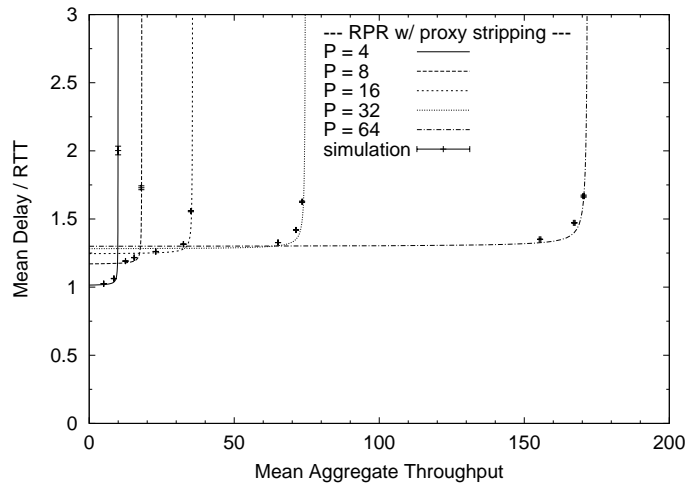

Fig. 15. Mean delay versus mean aggregate throughput of RPR with $P \in \{4, 8, 16, 32, 64\}$ proxy-stripping nodes and pretransmission coordination for uniform traffic with $N = 256$.

figure that with increasing P the mean delay increases. This is because with larger P more packets are proxy stripped, leading to an increased amount of control traffic and thus larger pretransmission coordination overhead. In the rest of the paper, we consider star subnetworks without pretransmission coordination.

5.B. Hot-Spot Traffic

Next we investigate RPR and the effect of proxy stripping on its throughput-delay performance under hot-spot traffic. Recall from Section 1 that hot-spot (hubbed) traffic is typically found in metro edge rings. We define our hot-spot traffic matrix as follows. Let node $i = 0$ be the hub node (hot spot). Each node i, $1 \leq i \leq N-1$, generates the same amount of traffic ρ, where $\rho \geq 0$. A given node i, $1 \leq i \leq N-1$, sends a generated packet to the hot spot with probability h, $0 \leq h \leq 1$, and to any other of the remaining $(N-2)$ nodes with equal probability $(1-h)/(N-2)$. To examine both symmetric and asymmetric hot-spot traffic, we introduce the parameter α which controls the traffic generated by the hot spot and the remaining $(N-1)$ nodes. Specifically, the amount of traffic generated by hot spot $i = 0$ and destined for any of the remaining $(N-1)$ nodes is equal to $\alpha h \rho$, where $0 \leq \alpha \leq 1$. The amount of traffic generated by node i, $1 \leq i \leq N-1$, is multiplied by $(1-\alpha)$. Thus, we have

$$\rho(0, j) = \alpha h \rho, \quad \text{if } 1 \leq j \leq N-1, \tag{46}$$

$$\rho(i, 0) = (1-\alpha) h \rho, \quad \text{if } 1 \leq i \leq N-1, \tag{47}$$

$$\rho(i, j) = (1-\alpha)(1-h)\frac{1}{N-2}\rho, \quad \text{if } 1 \leq i, j \leq N-1, \tag{48}$$

where $\alpha, h \in [0, 1]$. Table 3 shows different types of traffic used in the subsequent numerical investigations and the corresponding values of α and h.

<div align="center">

Table 3. Generic Traffic Model

Traffic Type	α	h
Symmetric uniform	0.5	$1/(N-1)$
Symmetric hot spot	0.5	1.0
Asymmetric hot spot (data distribution)	1.0	1.0
Asymmetric hot spot (data collection)	0	1.0

</div>

In this section, we concentrate on symmetric traffic with $\alpha = 0.5$. That is, a given node and the hub node generate the same amount of traffic destined for each other. In Figs. 16 and 17 we examine the throughput-delay performance of RPR without and with proxy stripping under hot-spot traffic and compare it with that obtained under uniform traffic for $N = 256$. Figure 16 illustrates the throughput-delay performance of RPR without proxy stripping for $h \in \{1/(N-1), 0.5, 1.0\}$. For uniform traffic, i.e., $h = 1/(N-1) = 1/255$, the maximum mean aggregate throughput is upper bounded by eight, as discussed above. However, for nonuniform traffic the performance of RPR decreases dramatically. For $h = 1.0$, i.e., when all nodes send packets only to the hub, the maximum aggregate throughput equals four, which is half of that obtained under uniform traffic. Also, we observe that for a mixed traffic scenario with $h = 0.5$, i.e., when 50% of the generated packets are destined to the hub while the other 50% are equally distributed among the remaining $(N-2)$ destination nodes, the throughput performance of RPR is still decreased significantly. The throughput deterioration of RPR under nonuniform traffic is due to the fact that packets traverse

more intermediate nodes and thus consume more bandwidth resources compared with uniform traffic. As a result, fewer nodes can transmit simultaneously, which translates into a decreased mean aggregate throughput.
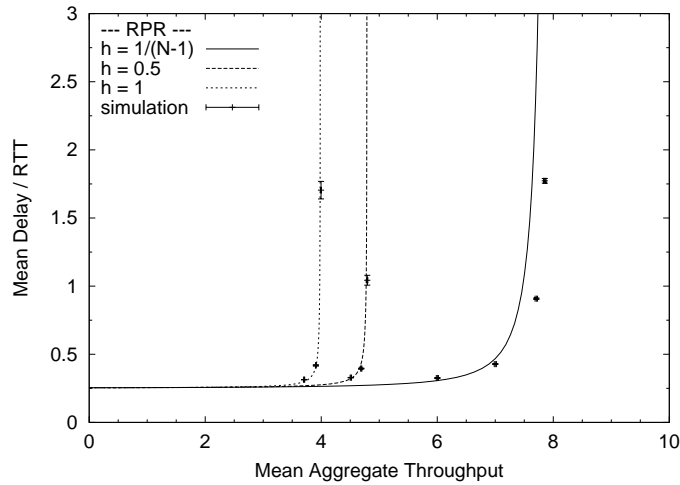

Fig. 16. Mean delay versus mean aggregate throughput of RPR without proxy stripping for symmetric hot-spot traffic with $h \in \{1/(N-1), 0.5, 1.0\}$, $\alpha = 0.5$, and $N = 256$.
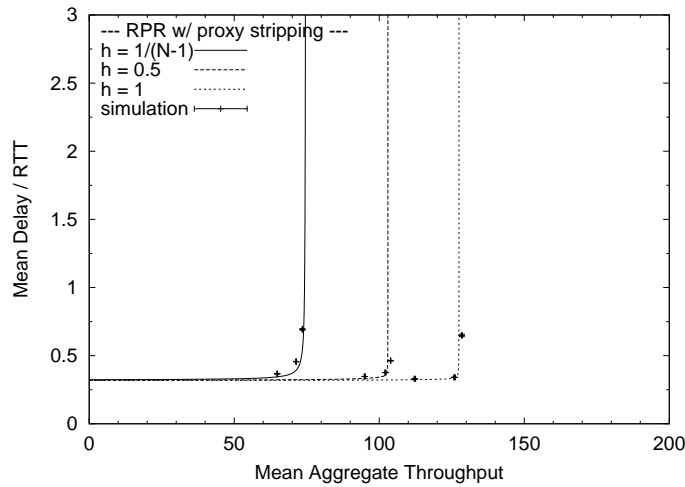

Fig. 17. Mean delay versus mean aggregate throughput of RPR with $P = 32$ proxy-stripping nodes for symmetric hot-spot traffic with $h \in \{1/(N-1), 0.5, 1.0\}$, $\alpha = 0.5$, and $N = 256$.

Figure 17 shows the throughput-delay performance of RPR using $P = 32$ proxy-stripping nodes for both uniform and nonuniform traffic. Under nonuniform traffic we observe the opposite behavior in RPR with proxy stripping compared with RPR without proxy stripping. We observe that, under nonuniform traffic, sending proxy-stripped traffic across the shortcuts of the star subnetwork increases the maximum mean aggregate throughput dramatically. Note that for $h = 1.0$ proxy stripping increases the maximum mean aggregate throughput of RPR by a factor of more than 30.

5.C. Asymmetric Traffic

Next, we examine asymmetric hot-spot traffic. In Figs. 18 and 19 we investigate the throughput-delay performance of RPR without and with proxy stripping under hot-spot traffic with $h = 1.0$ for $N = 256$. Again, in RPR with proxy stripping we set $P = 32$. In both figures we consider $\alpha \in \{0, 0.5, 1.0\}$. Recall that $\alpha = 0.5$ corresponds to symmetric traffic. The other two cases $\alpha = 0$ and $\alpha = 1.0$ represent asymmetric traffic between hub node and regular ring nodes. More precisely, with $\alpha = 0$ the hub generates no traffic while the remaining $(N-1)$ nodes generate only traffic destined for the hub. This traffic scenario corresponds to data collection. Conversely, with $\alpha = 1.0$ only the hub generates traffic for the remaining $(N-1)$ nodes while the latter ones are completely idle. This traffic scenario corresponds to data distribution. We observe that due to the symmetry of the architecture both data collection and data distribution achieve the same maximum mean aggregate throughput, which is half of that obtained under symmetric traffic. As shown in Fig. 18, for $\alpha \in \{0, 1.0\}$ the mean aggregate throughput of RPR without proxy stripping is not more than two, since the hub deploys two transceivers, one for each fiber ring. In contrast, in RPR with proxy stripping the mean aggregate throughput is more than 60 and thus dramatically larger than two for both data collection and distribution. This is because, apart from using the ring, the hub node also sends and receives data via the star subnetwork, leading to a dramatically increased mean aggregate throughput.

5.D. Dimensioning of Star Subnetwork

In this section, we investigate the forwarding burden caused by proxy stripping and the resultant capacity requirements of the star subnetwork in greater detail. Recall from Subsection 4.D that the star subnetwork was assumed to provide sufficient capacity to carry proxy-stripped traffic. In the following, we quantify the capacity requirements of the star subnetwork that must be met in order to avoid a bandwidth bottleneck. To this end, we consider proxy-stripping node $i = 0$ under both symmetric uniform and symmetric hot-spot traffic, i.e., $\alpha = 0.5$ and $h = 1/(N-1)$ or $h = 1.0$, respectively. To measure the capacity requirement of node $i = 0$, we use the ratio of the star transceiver load and the ring transceiver load. The star transceiver load at node $i = 0$ is identical to the amount of traffic $\rho_s(0)$ that arrives at the star transmit queue of node $i = 0$ (given by Eq. (38) of Subsection 4.D.3). The ring transceiver load at node $i = 0$ is identical to the amount of traffic that arrives at one of both ring transit queues of node $i = 0$. We choose the ring transit queue that belongs to the counterclockwise fiber ring. Thus, the ring transceiver load at node $i = 0$ is composed of all traffic coming from the transmit and transit queues of neighboring node $i = 1$. The ring transceiver load at node $i = 0$ is thus equal to the sum $\rho_t^{r-}(1) + \rho_t^{\mathrm{out}}(1) + \rho_r^{r-}(1) + \rho_r^{s-}(1)$ (where the individual terms are given by Eqs. (30), (31), (34), (37) of Subsection 4.D, respectively). Note that the ratio of the above explained star transceiver load and ring receiver load indicates the required star transmission rate normalized by the arrival rate of one ring. In other words, this ratio denotes the factor by which the star transceiver of a given proxy-stripping node has to operate faster than either of its ring transceivers in order to provide sufficient capacity in the star subnetwork. Thus, at each proxy-stripping node the star transceiver may have to operate at a line rate that is higher than the ring line rate if the ratio is larger than one. Alternatively, each proxy-stripping node may be equipped with more than one star transceiver, each operating at the same line rate as the ring transceivers, in order to provide sufficient transmission and reception capacity in the star subnetwork.

Figures 20 and 21 depict the ratio of the star transceiver load and the ring transceiver load at node $i = 0$ versus the number of nodes N for symmetric uniform and hot-spot traffic with $P \in \{4, 8, 16, 32, 64\}$. Note that under uniform traffic node $i = 0$ is one of P proxy-stripping nodes and thus represents the traffic present at the remaining $(P-1)$ proxy-
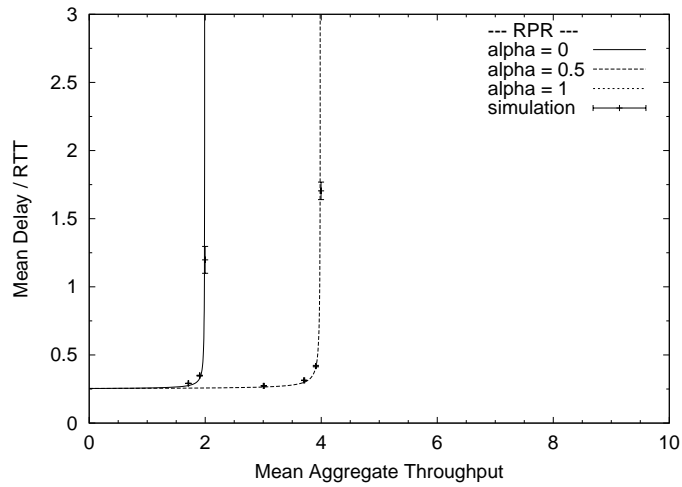
Fig. 18. Mean delay versus mean aggregate throughput of RPR without proxy stripping for asymmetric hot-spot traffic with $\alpha \in \{0, 0.5, 1.0\}$, $h = 1.0$, and $N = 256$.
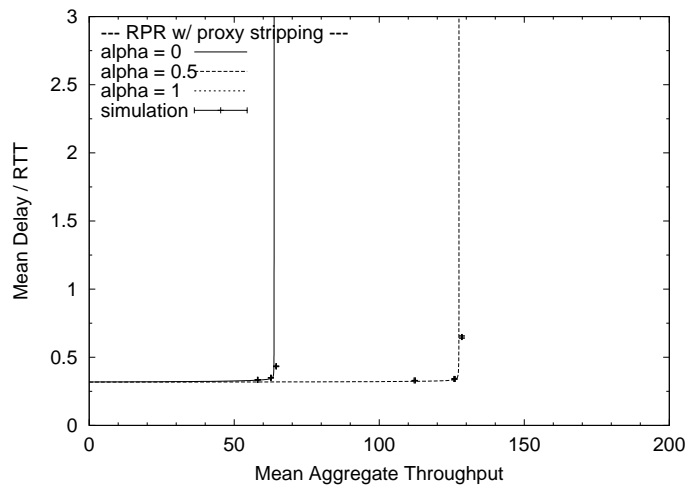

Fig. 19. Mean delay versus mean aggregate throughput of RPR with $P = 32$ proxy-stripping nodes for asymmetric hot-spot traffic with $\alpha \in \{0, 0.5, 1.0\}$, $h = 1.0$, and $N = 256$.

stripping nodes as well. From Fig. 20 we observe that the ratio increases for larger P under uniform traffic. This is because with an increasing P more nodes are attached to the star subnetwork. Therefore, more nodes communicate with one another via the star subnetwork, resulting in an increased star traffic volume. Also, we observe that for a given P the ratio decreases with increasing N. This is due to the fact that with P fixed and increasing N more nodes communicate with each other via the ring rather than the star subnetwork. As a consequence, the ring traffic increases and the star traffic decreases, leading to a smaller ratio. In summary, for uniform traffic it appears to be reasonable to use a moderate number of proxy-stripping nodes P compared with the number of nodes N. Thus the traffic load is well balanced between the ring and the star subnetwork. Moreover, choosing a moderate number of proxy-stripping nodes P requires fewer dark fibers and star transceivers, each operating at a line rate that is slightly larger than that of the ring transceivers.

Next, let us consider the ratio under hot-spot traffic, as shown in Fig. 21. Again, we observe that with increasing P the ratio becomes larger. Note, however, that under hot-spot traffic the ratio is significantly larger than under uniform traffic. This is because now all nodes have traffic destined only for hot-spot node $i = 0$, which in terms of hops is best reached via the shortcuts of the star subnetwork. To use these shortcuts, regular ring nodes send their hot-spot traffic toward their closest proxy-stripping node, which then transmits the traffic directly to node $i = 0$ across the star subnetwork. Due to the lack of traffic between regular nodes the utilization of the ring is rather small compared with the star subnetwork. As a result, the ratio is much larger under hot-spot than under uniform traffic. Furthermore, we observe from Fig. 21 that for a given P the ratio does not decrease for increasing N. Instead, for a given P there are certain values of N that provide a smaller or larger ratio, where the difference between the small and large ratios becomes more pronounced with increasing P. Note that for each value of P the oscillations between small and large ratios become gradually smoother with increasing N. The reason for this is as follows. The number of regular ring nodes next to hub node $i = 0$ is equal to $(N/P - 1)$ in each direction. Among these nodes, $\lceil (N/P - 1)/2 \rceil$ nodes send their packets to node $i = 0$ via the ring while the remaining $\lfloor (N/P - 1)/2 \rfloor$ make use of the star subnetwork. Now, by gradually increasing $(N/P - 1)$ every second node sends its hot-spot traffic to node $i = 0$ either directly on the ring or via the star subnetwork. As a result, only one of the transceiver loads at node $i = 0$ is increased, i.e., either the star or the ring transceiver load, while the other one remains unchanged, resulting in oscillations of the ratio. The oscillations become smoother because the relative traffic contribution of each newly added node becomes smaller for increasing $(N/P - 1)$.

Given the number of ring nodes N, number of proxy-stripping nodes P, and traffic type (uniform, nonuniform), the star subnetwork can be designed such that the above mentioned ratio of star transceiver and ring transceiver loads is satisfied. For a small ratio and/or small P the star subnetwork may consist of a PSC with one star transceiver at each proxy-stripping node, whereas for a large ratio and/or large P each proxy-stripping node may be equipped with an array of transceivers attached to a wavelength-routing AWG-based star subnetwork that provides a large number of communication channels because of extensive spatial wavelength reuse, as discussed in Section 3.

6. Conclusions

Optical metropolitan area ring networks with destination stripping and shortest path routing such as RPR will be primarily used in metro interconnected rings that consist of metro core and metro edge rings whose traffic demands are completely different. We have shown by means of probabilistic analysis and verifying simulations that the throughput-delay performance of RPR decreases dramatically under nonuniform symmetric and asymmetric traffic,
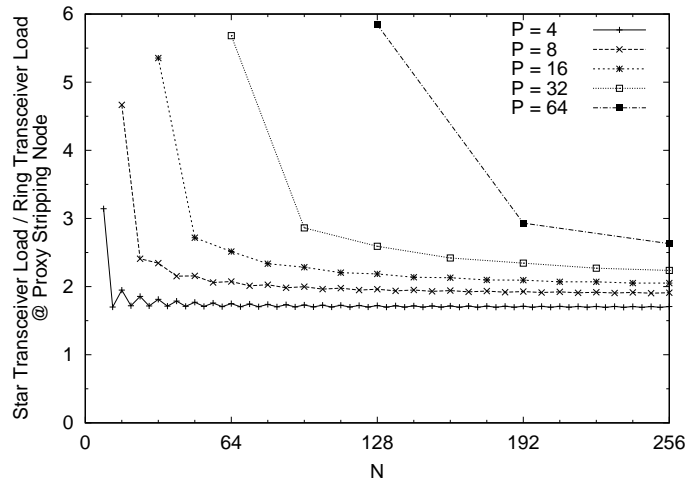
Fig. 20. Ratio of star transceiver and ring transceiver loads versus number of nodes N at proxy-stripping node $i = 0$ for symmetric uniform traffic [$\alpha = 0.5$, $h = 1/(N-1)$] with $P \in \{4, 8, 16, 32, 64\}$.
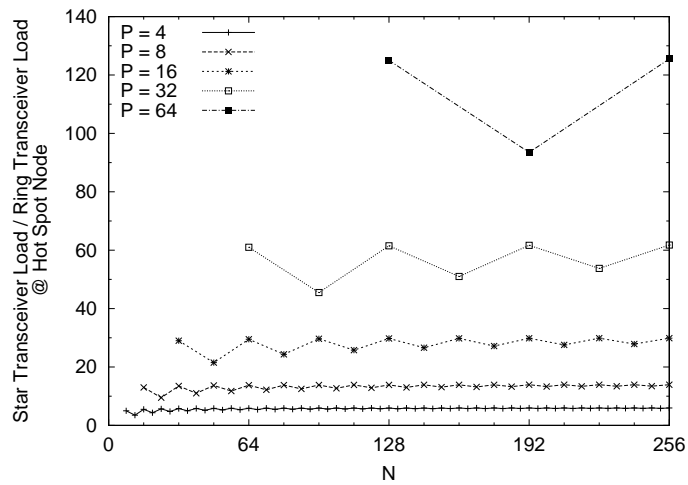

Fig. 21. Ratio of star transceiver and ring transceiver loads versus number of nodes N at hot-spot node $i = 0$ for symmetric hot-spot traffic ($\alpha = 0.5$, $h = 1.0$) with $P \in \{4, 8, 16, 32, 64\}$.

which is typically found in metro edge rings. In metro edge rings with hot-spot traffic demands the maximum aggregate throughput of RPR is reduced to half of that obtained under uniform traffic. To mitigate this shortcoming of RPR, we have described and evaluated the proxy-stripping technique that can be used to improve the throughput-delay performance of RPR both under uniform and hot-spot traffic significantly. For uniform traffic, interconnecting 32 of 256 ring nodes via a star subnetwork increases the maximum mean aggregate throughput of RPR by a factor of almost ten.

We have seen that the number of proxy-stripping nodes P must be chosen properly. If P is chosen too small, the fiber links close to the proxy-stripping nodes become congested and form a bottleneck, resulting in an underutilized star subnetwork and a deteriorated overall throughput-delay performance. One approach to alleviate this congestion might be the use of transparent proxy stripping, where ring nodes are not aware of proxy-stripping nodes and thus do not create this type of hot-spot traffic on the ring. On the other hand, a large P requires too many star transceivers and dark fibers for interconnecting the proxy-stripping nodes. A moderate number of proxy-stripping nodes appear to provide a reasonable trade-off between throughput-delay performance improvement of RPR and costs.

The star subnetwork is best built by using dark fibers, which are abundantly available in metropolitan regions. Depending on the number of ring nodes, number of proxy-stripping nodes, amount and type (uniform, nonuniform) of traffic demands the star subnetwork has to be designed not only to provide enough capacity to proxy-stripped and shortcut traffic but also to balance the traffic loads on both rings and the star subnetwork. Apart from the design of an efficient star subnetwork, fairness control in proxy-stripping ring-star networks is another avenue for future research. In our ongoing work we are investigating the protection and restoration in ring networks with proxy stripping.

Appendix A.

In this appendix we analyze the mean waiting time in the star transmit queue of proxy-stripping node i, where $i = 0, n, 2n, \ldots, (N - n)$. Let the continuous-time process $\{N(t)\}_{t \geq 0}$ denote the system size (i.e., all packets waiting in the queue and the packet currently being transmitted) at time t. Note that $\{N(t)\}_{t \geq 0}$ is a non-Markovian process. Next, we embed a Markov chain on $\{N(t)\}_{t \geq 0}$. At any given time t we consider a pair of random variables $N(t)$, the number of packets in the system, and $X(t)$, the transmitting time already spent on the packet under service, if any. The vector $\{N(t), X(t)\}_{t \geq 0}$ is a continuous-time Markov process. We observe the system at the end of each packet transmission, which we call departure instant henceforth. Let t_n, $n \in \mathbb{N}$, be the departure instants and $N(t_n)$ denote the number of transmitted packets at time instant t_n. For our queueing system with Poisson arrivals we obtain the following properties:

- The probability that an arriving packet finds n packets in a given star transmit queue equals the probability that n packets have already been transmitted. In equilibrium this probability is also equal to the probability that the number of packets in the system equals n.

- The transitions of the process occur at the departure instants t_n. Thus, $\{N(t_n)\}_{t \geq 0}$ is a Markov chain.

Next, let F_L denote the distribution of the packet transmission time T_p. The Laplace transform of F_L is then given by

$$L^*(\tau) = \int_0^\infty e^{-\tau t} \mathrm{d}F_L(t) \qquad \text{with } -L^{*(1)}(0) = E[T_p] =: \frac{1}{\mu} \tag{A1}$$

independent of i. Let $A(i)$ denote the number of arrivals during the service (transmission) time of a given packet. Conditioned on that duration, we get

$$k_r(i) := P(A(i) = r) = \int_0^\infty \frac{\exp[-\lambda_s(i)t][\lambda_s(i)t]^r}{r!} dF_L(t), \quad r = 0, 1, \dots, \tag{A2}$$

where $\lambda_s(i) = \rho_s(i)/E[T_p]$ and $\rho_s(i)$ is given in Eq. (38). By using the probability generating function

$$G_A^{(i)}(\tau) = \sum_{r=0}^\infty k_r(i)\tau^r = \int_0^\infty \exp\{-[\lambda_s(i) - \lambda_s(i)\tau]t\} dF_L(t) = L^*(\lambda_s(i) - \lambda_s(i)\tau), \tag{A3}$$

we obtain

$$E[A] = G_A^{(i)\prime}(1) = -\lambda_s(i)L^{*(1)}(0) = \frac{\lambda_s(i)}{\mu} =: \rho(i). \tag{A4}$$

With X_n denoting the number of packets transmitted prior to the nth packet and A_n denoting the number of packets that arrive during the service (transmission) time of the nth packet we obtain the following Lindley equation

$$X_{n+1} = \begin{cases} X_n - 1 + A_{n+1} & \text{if } X_n \geq 1 \\ A_{n+1} & \text{if } X_n = 0 \end{cases}. \tag{A5}$$

Note that A_n is independent of n, i.e., $A_n = A$ for all n. Next, let p_{ij} be the transition probabilities of the denumerable Markov chain $\{X_n\}_{n \geq 0}$, which are given by

$$p_{ij} = P(X_{n+1} = j \mid X_n = i). \tag{A6}$$

Clearly,

$$p_{ij} = \begin{cases} k_{j-i+1} & \text{if } i \geq 1, j \geq i - 1 \\ 0 & \text{if } i \geq 1, j < i - 1 \end{cases}, \tag{A7}$$

and $p_{0j} = k_j$, where $j \geq 0$. Note that the transition probability matrix is irreducible and aperiodic. It can be shown that the Markov chain is persistent nonnull and hence ergodic. According to the ergodic theorem the steady-state probabilities are given by

$$p_j := \lim_{n \to \infty} p_{ij}^{(n)}, \quad j = 0, 1, 2, \dots, \tag{A8}$$

independent of the initial state i. Hence, the probability generating function is given by

$$G_{(p_j)_{j \geq 0}}^{(i)}(\tau) = \frac{[1 - G_A^{(i)\prime}(1)](1 - \tau)G_A^{(i)}(\tau)}{G_A^{(i)}(\tau) - \tau}, \tag{A9}$$

and by setting $G_A^{(i)\prime} = \rho(i)$ we get for $0 < \rho(i) < 1$

$$G_{(p_j)_{j \geq 0}}^{(i)}(\tau) = \frac{[1 - \rho(i)](1 - \tau)L^*(\lambda_s(i) - \lambda_s(i)\tau)}{L^*(\lambda_s(i) - \lambda_s(i)\tau) - \tau}, \tag{A10}$$

which is known as the generalized Pollaczek–Khinchine formula. Let $W_q(i)$ denote the waiting time in the star transmit queue and let $W_{q,i}(t)$ denote its distribution function. From Eq. (A10) we then obtain, for $\rho(i) < 1$,

$$W_{q,i}^*(\tau) = \frac{\tau(1 - \rho(i))}{\tau - \lambda_s(i)[1 - L^*(\tau)]}, \tag{A11}$$

which is known as the Pollaczek–Khinchine transform formula. To get the moments we differentiate this formula

$$L^{*(k)}(0) = (-1)^k E\left[T_p^k\right]; \quad k = 1, 2, \ldots.$$

With L'Hospital, we finally get

$$E\left[W_q(i)\right] = \frac{\lambda_s(i)}{2(1-\rho(i))} E\left[T_p^2\right] = \frac{\lambda_s(i)}{2(1-\rho(i))}\left(\mathrm{var}\left[T_p\right] + \frac{1}{\mu}\right). \qquad (A12)$$

Acknowledgments

References and Links

[1] M. Maier, *Metropolitan Area WDM Networks—An AWG Based Approach* (Kluwer Academic, 2003).

[2] M. Herzog, M. Maier, and M. Reisslein, "Metropolitan area packet-switched WDM networks: a survey on ring systems," IEEE Commun. Surv. **6**(2), 2–20 (2004).

[3] IEEE, "Draft P802.17, v. 3.0: resilient packet ring," (November 2003).

[4] F. Davik, M. Yilmaz, S. Gjessing, and N. Uzun, "IEEE 802.17 resilient packet ring tutorial," IEEE Commun. Mag. **42**(3), 112–118 (2004).

[5] P. Yuan, V. Gambiroza, and E. Knightly, "The IEEE 802.17 media access protocol for high-speed metropolitan-area resilient packet rings," IEEE Netw. **18**(3), 8–15 (2004).

[6] S. Spadaro, J. Solé-Pareta, D. Careglio, K. Wajda, and A. Szymański, "Positioning of the RPR standard in contemporary operator environments," IEEE Netw. **18**(2), 35–40 (2004).

[7] P. Yue, Z. Liu, and J. Liu, "High performance fair bandwidth allocation algorithm for resilient packet ring," in *Proceedings of the International Conference on Advanced Information Networking and Applications (AINA)* (IEEE Computer Society, 2003), pp. 415–420.

[8] X. Zhou, G. Shi, H. Fang, and L. Zeng, "Fairness algorithm analysis in resilient packet ring," in *International Conference on Communication Technology Proceedings* (IEEE, 2003), Vol. 1, pp. 622–624.

[9] V. Gambiroza, P. Yuan, L. Balzano, Y. Liu, S. Sheafor, and E. Knightly, "Design, analysis, and implementation of DVSR: a fair, high performance protocol for packet rings," IEEE/ACM Trans. Netw. **12**(1), 85–102 (2004).

[10] N. Ghani, J.-Y. Pan, and X. Cheng, "Metropolitan optical networks," Opt. Fiber Telecommun. **IVB**, 329–403 (2002).

[11] W. Aiello, S. N. Bhatt, F. R. K. Chung, A. L. Rosenberg, and R. K. Sitaraman, "Augmented ring networks," IEEE Trans. Parallel Distrib. Syst. **12**(6), 598–609 (2001).

[12] I. Rubin and H.-K. Hua, "An all-optical wavelength-division meshed-ring packet-switching network," in *Proceedings of IEEE INFOCOM* (IEEE, 1995), Vol. 3, pp. 969–976.

[13] I. Rubin and H.-K. Hua, "SMARTNet: an all-optical wavelength-division meshed-ringpacket-switching network," in *IEEE Global Telecommunications Conference, 1995. GLOBECOM '95* (IEEE, 1995), Vol. 3, pp. 1756–1760.

[14] M. S. Goodman, "Multiwavelength networks and new approaches to packet switching," IEEE Commun. Mag. **27**(10), 27–35 (1989).

[15] M. S. Goodman, "Optical networks: new approaches to interconnection and switching," in *LEOS Summer Topical on Optical Multiple Access Networks, 1990. Conference Digest* (IEEE, 1990), pp. 13–14.

[16] A. M. Hill, M. Brierley, R. M. Percival, R. Wyatt, D. Pitcher, K. M. I. Pati, I. Hall, and J.-P. Laude, "Multiple–star wavelength–router network and its protection strategy," IEEE J. Sel. Areas Commun. **16**, 1134–1145 (1998).

[17] W.-P. Lin, M.-S. Kao, and S. Chi, "The modified star–ring architecture for high–capacity subcarrier multiplexed passive optical networks," J. Lightwave Technol. **19**, 32–39 (2001).

[18] M. Herzog, M. Maier, and A. Wolisz, "RINGOSTAR: an evolutionary AWG based WDM upgrade of optical ring networks," J. Lightwave Technol. **23**, 1637–1651 (2005).

[19] B. Mukherjee, "WDM–based local lightwave networks part i: single-hop systems," IEEE Netw. **6**(3), 12–27 (1992).

[20] M. Maier, M. Reisslein, and A. Wolisz, "Towards efficient packet switching metro WDM networks," Opt. Netw. Mag. **3**(6), 44–62 (2002).

[21] M. Maier, and M. Reisslein, "AWG-based metro WDM networking," IEEE Commun. Mag.**42**(11), S19–S26 (2004).

[22] H.-S. Yang, M. Herzog, M. Maier, and M. Reisslein, "Metro WDM networks: performance comparison of slotted ring and awg star networks," IEEE J. Sel. Areas Commun. **22**, 1460–1473 (2004).

[23] W. Bux and M. Schlatter, "An approximate method for the performance analysis of buffer insertion rings," IEEE Trans. Commun. **COM-31**(1), 50–55 (1983).

[24] C. Fraleigh, S. Moon, B. Lyles, C. Cotton, M. Khan, D. Moll, R. Rockell, T. Seely, and C. Diot, "Packet-level traffic measurements from the Sprint IP backbone," IEEE Netw. **17**(6), 6–16 (2003).